IOPscience iopscience.iop.org

Home Search Collections Journals About Contact us My IOPscience

Chemical chaos and self-organization

This article has been downloaded from IOPscience. Please scroll down to see the full text article.

1990 J. Phys.: Condens. Matter 2 SA47

(http://iopscience.iop.org/0953-8984/2/S/005)

View the table of contents for this issue, or go to the journal homepage for more

Download details:
IP Address: 129.252.86.83
The article was downloaded on 27/05/2010 at 11:15

Please note that terms and conditions apply.

J. Phys.: Condens. Matter **2** (1990) SA47–SA62. Printed in the UK

Chemical chaos and self-organization

G Nicolis
Faculté des Sciences, Université Libre de Bruxelles, Campus Plaine, CP 231, Boulevard du Triomphe, B-1050 Bruxelles, Belgium

Received 23 August 1990

Abstract. The onset of chaotic behaviour and space patterning in chemically reacting systems is analysed. Special emphasis is placed on the specificities of chemical dynamics as compared to other branches of physical sciences giving rise to chaos and self-organization and on the role of the size of the system as a universal bifurcation parameter.

1. Introduction

It is by now well established that, when operating under far-from-equilibrium constraints, large classes of chemical reactions may give rise to a variety of complex phenomena such as periodic, quasi-periodic and chaotic oscillations and spatial or spatio-temporal patterns [1, 2]. In this paper we survey progress achieved in recent years in the understanding of this behaviour.

In order to focus on phenomena arising entirely from the chemical kinetics, we shall limit ourselves to isothermal systems in mechanical equilibrium and discard, therefore, heat transfer and hydrodynamic motion. The resulting system is described to a very good approximation by the reaction–diffusion equations,

$$\partial X_i/\partial t = v_i(X_i, \ldots, X_n; \lambda, \mu, \ldots) + D_i \nabla^2 X_i \qquad (i = 1, \ldots, n) \tag{1}$$

where X_i is a set of variables describing the composition of the mixture; v_i is the rate of a change of X_i due to the chemical reactions; $\lambda, \mu, \ldots$ are parameters (rate constants etc) built in the system; and D_i is the diffusion coefficient of species i in the medium (for simplicity cross-diffusion effects are neglected, a restriction that is valid as long as the reacting mixture behaves as an ideal system). It is through this latter coefficient as well as through the parameters $\lambda, \mu, \ldots$ that the nature of the host medium, and particularly the possibility of it being in the liquid state, is likely to affect the behaviour of our reaction–diffusion system.

There are two important features of equations (1) that make chemical kinetics special among other fields of physical sciences.

(i) v_i are, typically, non-linear functions of the composition variables owing to the presence of cooperative effects like autocatalysis or inhibition, which are ubiquitous in chemistry. These effects are acting spontaneously everywhere in the system. They therefore subsist in the limit of a uniform medium, in which diffusion can be discarded.

0953-8984/90/SA0047 + 16 $03.50 © 1990 IOP Publishing Ltd

This latter limit can be achieved in the laboratory through an effective stirring mechanism. Equations (1) reduce then to a system of non-linear ODEs

$$dX_i/dt = v_i(X_i, \ldots, X_n; \lambda, \mu, \ldots) \tag{2}$$

which contain practically all the tremendous variety of complex behaviour suggested by the mathematical analysis of non-linear dynamical systems with a small number of degrees of freedom [3]. In other words, complexity in chemistry is not necessarily induced by the spatial degrees of freedom like in hydrodynamics: it may arise solely from the intrinsic non-linearities of the kinetics. Furthermore, chemical dynamics is generated by purely dissipative processes, in contrast to hydrodynamics or electromagnetic processes where inertia plays an important role. In short, chemical reactions provide one of the few authentic physical illustrations of low-dimensional dissipative dynamical systems.

(ii) Suppose next that the system is not stirred: diffusion is automatically switched on, and states corresponding to an inhomogeneous distribution of X_i in space are created. Before attempting any quantitative evaluation of the properties of such states, let us follow a simple dimensional argument. Among the parameters present in equations (1), let us focus our attention on a typical diffusion coefficient, D, and a typical rate constant, k. From these two quantities we can construct a combination $l_c = (D/k)^{1/2}$ having the dimensions of length and being of completely intrinsic origin. This suggests that reaction–diffusion systems should be capable of undergoing spontaneous symmetry-breaking transitions leading to states endowed with intrinsic characteristic lengths. This is to be contrasted with hydrodynamics where length scales involve, among other factors, the system size.

Having identified the main features that distinguish reaction–diffusion systems from other systems giving rise to bifurcations and non-linear dynamics, we shall now proceed to a brief account of some selected topics, by placing special emphasis on open questions and recent developments. We shall deal, successively, with mixed-mode oscillations and homoclinic chaos in well-stirred systems; symmetry breaking and pattern formation in spatially distributed systems; and the microscopic aspects of chemical instabilities.

2. Mixed-mode oscillations and homoclinic chaos in well-stirred systems

When a chemical reaction takes place in an open, well-stirred reactor, the time evolution of the concentration is described by a system of non-linear first-order ODEs (equation (2)). In this case the evolution can be embedded in a finite-dimensional phase space of dimension equal to the number of chemical species involved in the reaction. The advances of computer technology, in particular the advent of graphic terminal technology on the one hand, and phase space methods on the other, have led to important progress in the analysis of far-from-equilibrium chemical reactions in time-dependent dynamical regimes which have been classified into periodic, quasiperiodic and chaotic behaviour. Moreover several bifurcation mechanisms for transition from periodic to chaotic behaviour have been observed and studied in detail such as the Feigenbaum period doubling cascade, the intermittency transition, the quasiperiodic route to chaos and the homoclinic tangencies. The latter, discovered in the mid-sixties and early seventies by Sil'nikov and co-workers [4], have in fact been among the first known examples of bifurcations leading to chaos.

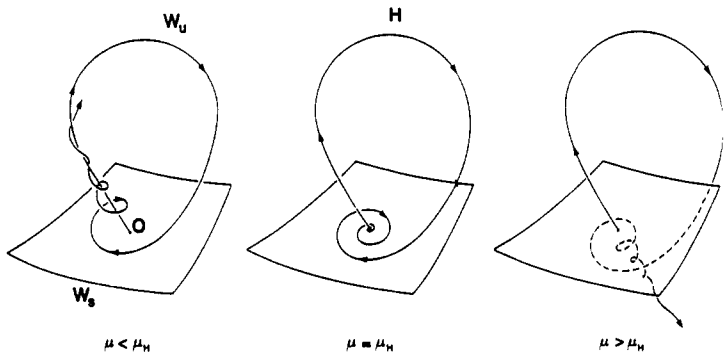

Figure 1. Phase portrait of a homoclinic tangency to a saddle focus (O) in a three-dimensional phase space, before ($\mu < \mu_H$), at ($\mu = \mu_H$) and after ($\mu > \mu_H$) the bifurcation. W_s and W_u are the stable and unstable manifolds of (O). The homoclinic orbit (H) exists at the tangency ($\mu = \mu_H$).

Homoclinic tangencies are very common in low-dimensional ODEs, in particular in chemical kinetics. A homoclinic tangency will occur in the phase space if two conditions are satisfied:

(i) There exists an invariant set, i.e. a fixed point, a periodic orbit or a Cantor set of orbits, that is of the saddle type. Accordingly trajectories escape from the invariant set along the unstable manifold while other trajectories are convergent to the invariant set along the stable manifold.

(ii) The unstable manifold is tangential to the stable manifold at a critical parameter value $\mu = \mu_H$.

This latter condition implies that bifurcations occur in the vicinity of a homoclinic tangency. Not all homoclinic tangencies lead to chaotic behaviour. For instance, when a tangency occurs in two dimensions it generates a single periodic orbit. However, general conditions for emergence of homoclinic chaos have been proved. We shall now turn to a description of some typical results, taking as an illustrative example the case of homoclinic orbits associated with a fixed point in a system involving three variables.

The geometry of this homoclinic bifurcation is depicted in figure 1. We assume that there exists a fixed point which is a saddle-focus with linear stability eigenvalues $(\rho \pm i\omega, \lambda)$. The stable manifold is two-dimensional while the unstable one is one-dimensional. At the critical parameter value $\mu = \mu_H$, the unstable manifold is included into the stable one and forms the homoclinic orbit. However, this situation breaks down away from criticality. We then have the following general results [4–6]:

(i) Sil'nikov theorem: provided $|\rho/\lambda| < 1$, there exist uncountably many non-periodic orbits.

(ii) As shown in figure 2, the orbits successively perform $(\ldots, p^{i-1}, p^i, p^{i+1}, \ldots)$ half-turns around the saddle-focus, interrupted by bursts. Accordingly, they were named mixed-mode oscillations because they are composed of a mixture of small peaks followed by a large peak. The time spent between two bursts is $\tau^i = \pi p^i/\omega + \tau_H$ where τ_H is the time for a burst. Most of these orbits are chaotic, but there also exist single-circuit periodic orbits of the type $(\ldots, p, p, p, \ldots)$ and of period $T = \pi p/\omega + \tau_H$. These orbits

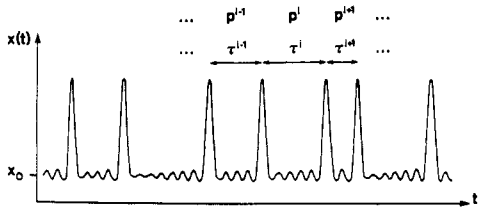

Figure 2. Typical time evolution of a kinetic variable $x(t)$ in Sil'nikov chaos. The small growing oscillations (p^i) are interrupted by bursts, forming a random sequence of time intervals (τ^i). The bursts correspond to a circuit in the vicinity of the underlying homoclinic orbit.

are of relaxation type and are very different from the quasi-sinusoidal oscillations born in the Hopf bifurcation.

(iii) The above single-circuit periodic orbits appear in pairs via tangent bifurcations. The bifurcation points $\{\mu_n^{\pm}\}$ accumulate geometrically to $\mu = \mu_H$ according to

$$\lim_{n\to\infty} \frac{\mu_n^{\pm} - \mu_{n-1}^{\pm}}{\mu_{n+1}^{\pm} - \mu_n^{\pm}} = e^{2\pi|\rho/\omega|} \tag{3}$$

and their period increases to infinity as $\mu \to \mu_H$.

Remarks

(*a*) Sil'nikov's homoclinicity to a saddle focus is generic in two-parameter space near a doubly degenerate bifurcation of a fixed point with eigenvalues $(\pm i\omega, 0)$ in the case where the co-dimension two vector field is described by the normal form

$$\dot{q} = i\omega q + (\alpha + i\beta)zq + O(3) \qquad \dot{z} = -z^2 - |q|^2 + O(3)$$

where $q = x + iy$ and $0 < \alpha < 2$. Topological chaos is thus allowed arbitrarily close to the critical vector field, together with the aforementioned bifurcations.

(*b*) The bifurcation accumulation rate (3) at the homoclinic tangency is to be compared with the accumulation rate of period doublings in the Feigenbaum cascade where

$$\lim_{n\to\infty} \frac{\mu_n - \mu_{n-1}}{\mu_{n+1} - \mu_n} = 4.669\,2016\ldots \tag{4}$$

which is a universal number [7]. In contrast, the quantitative features of the homoclinic tangency depend on the eigenvalues of the saddle-focus.

Sil'nikov homoclinic tangency (and its heteroclinic variant) has been observed in the Rössler model, in the Lorenz model and the associated Haken model of lasers, in the spin-wave turbulence model, in double-diffusive convection models, in three variable Lotka–Volterra models, in models of non-linear wave modulation, in the nerve impulse propagation model and in models of heterogeneous catalysis, as well as in isothermal chemical kinetic models.

In particular, the following kinetic model, satisfying the mass-action law, has been shown to give rise to homoclinic chaos [5]:

$$\begin{aligned} \dot{X} &= X(dX - fY - Z + g) \\ \dot{Y} &= Y(X + sZ - l) \\ \dot{Z} &= (1/\varepsilon)(X - aZ^3 + bZ^2 - cZ). \end{aligned} \tag{5}$$

This system presents a homoclinic tangency to a saddle-focus at the parameter values

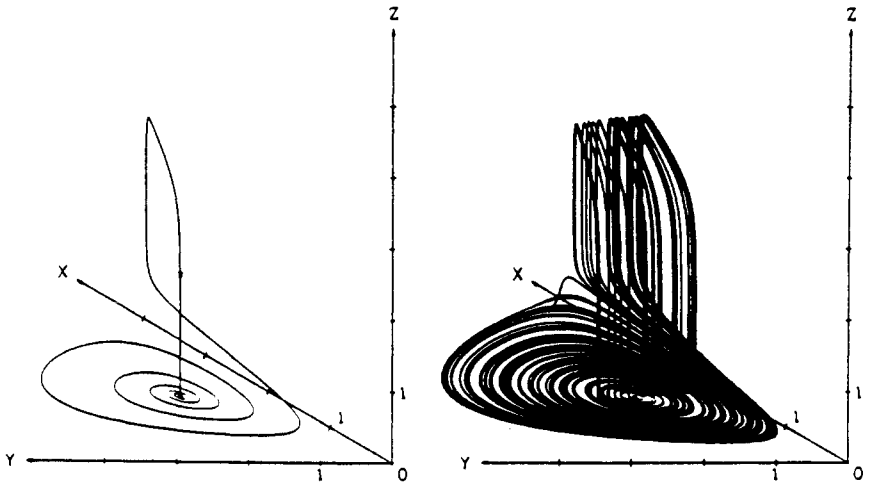

Figure 3. The homoclinic orbit of the chaotic attractor of the kinetic model (5) at $d = 0.51$ and $l = 1.339$.

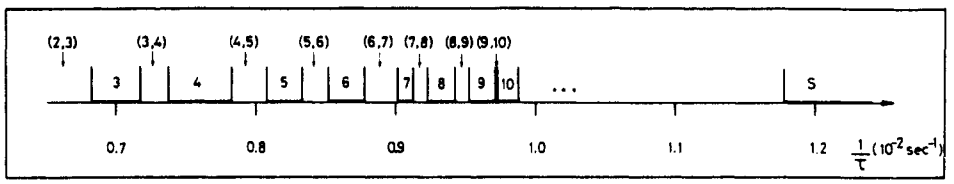

Figure 4. Complex bifurcation sequence of mixed-mode oscillations for the model (6) of the Belousov–Zhabotinski reaction proposed by Showalter *et al* (from [8]).

$a = 0.5$, $b = 3$, $c = 5$, $\varepsilon = 0.01$, $f = 0.5$, $g = 0.6$, $s = 0.3$. Figure 3 shows the homoclinic orbit at $d = 0.51$ and $l = 1.339$, embedded in a chaotic attractor. At homoclinicity, the stability eigenvalues of the saddle-focus are $\rho = 0.081$, $\omega = 1.064$, $\lambda = -332.4$. Note the stiffness of the differential equations (5) due to the smallness of parameter $\varepsilon = 0.01$. This kinetic model provided the first evidence for the possibility of Sil'nikov homoclinic chaos and the associated mixed-mode oscillations in far-from-equilibrium chemical reactions.

Complex bifurcation sequences of mixed-mode oscillation and a Sil'nikov homoclinic orbit were also observed in a model of the Belousov–Zhabotinski reaction by Showalter *et al* [8] who proposed the following kinetic scheme:

$$\begin{aligned} &A + Y \leftrightarrow X + P && X + Y \leftrightarrow 2P \\ &A + X \leftrightarrow 2W && C + W \leftrightarrow X + Z \\ &2X \leftrightarrow A + P && Z \rightarrow gY + C \end{aligned} \qquad (6)$$

with $A = BrO_3^-$, $C = M_{red}$, $P = HOBr$, $W = BrO_2^{\cdot}$, $X = HBrO_2$, $Y = Br^-$, $Z = M_{ox}$. The bifurcation sequence of mixed-mode oscillation for varying inverse residence times (τ) is depicted in figure 4. The periodic windows are labelled by single integers n when the oscillation is composed of n small peaks followed by a large one, and by pairs of

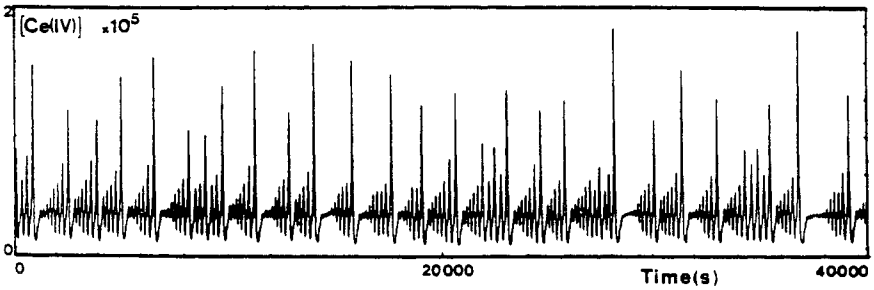

Figure 5. Experimental time evolution of the concentration of Ce^{IV} in the Belousov–Zhabotinski reaction, showing a typical homoclinic chaos: an oscillatory instability causes the growth of the small oscillations followed by the homoclinic reinjection (adapted from [9]).

integers (m, n) when the oscillation contains m small peaks followed by a large peak followed then by n small peaks etc. The number of small peaks in the pattern increases with $1/\tau$ until a transition to a stationary behaviour (S) takes place through a complex bifurcation sequence very similar to those occurring near the homoclinic tangency.

Experimental evidence of homoclinic chaos was provided by Argoul *et al* [9] in the Belousov–Zhabotinski reaction. They observed a homoclinic reinjection mechanism to a fixed point of saddle-focus type (see figure 5). Homoclinic chaos was also experimentally observed in heterogeneous catalysis, as well as in electrochemical deposition [10].

We conclude this section with the remark that homoclinic chaos appears to be a mechanism which is shared by a large variety of dynamical systems of interest in chemistry. They have in common the fact that a stationary instability competes with an oscillatory one leading to chaos.

3. Symmetry breaking and pattern formation

In the absence of stirring, far-from-equilibrium patterns can appear in chemically reacting systems as a result of diffusion-induced instabilities [1]. Historically, this mechanism was first proposed by Turing in 1952 as a model of morphogenesis [11].

For a reaction–diffusion system like

$$\partial \boldsymbol{X}/\partial t = \boldsymbol{v}(\boldsymbol{X}, \lambda) + \mathbf{D}\nabla^2 \boldsymbol{X} \tag{7}$$

(with $\boldsymbol{X} = (X_1, \ldots, X_n)$) the dissipative structure emerges from the uniform steady state solution,

$$\boldsymbol{v}(\boldsymbol{X}_0, \lambda) = 0 \tag{8}$$

given the boundary conditions $\boldsymbol{X} = \boldsymbol{X}_0$ or $\boldsymbol{n} \cdot \nabla \boldsymbol{X} = 0$. The linear stability analysis provides the critical parameter values where small-amplitude perturbations around $\boldsymbol{X}_0$ become unstable:

$$\boldsymbol{X} = \boldsymbol{X}_0 + \boldsymbol{x}(\boldsymbol{r}, t) \tag{9}$$

with $\boldsymbol{x}$ the solution of

$$\partial \boldsymbol{x}/\partial t = ((\partial \boldsymbol{v}/\partial \boldsymbol{X})(\boldsymbol{X}_0) + \mathbf{D}\nabla^2)\boldsymbol{x}. \tag{10}$$

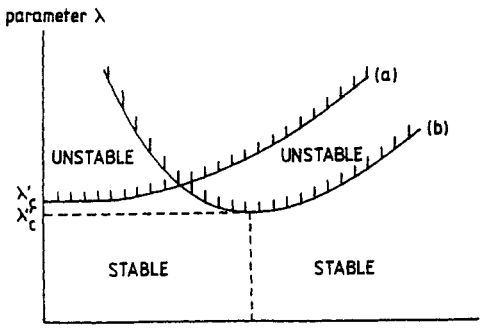

Figure 6. Lines of marginal stability in the plane of the parameter λ against the wavenumber k_m, for the temporal instability starting at $(\lambda_c', k_m = 0)$ and for the space-symmetry-breaking instability starting at $(\lambda_c'', k_m = k_{m_c})$.

This equation admits solutions of the form

$$\boldsymbol{x} = \boldsymbol{C}_m \, \mathrm{e}^{\omega_m t} \varphi_m(\boldsymbol{r}) \tag{11a}$$

where

$$\nabla^2 \varphi_m = -k_m^2 \varphi_m. \tag{11b}$$

The characteristic equation is then

$$\det |(\partial \boldsymbol{v}/\partial \boldsymbol{X})(\boldsymbol{X}_0) - k_m^2 \mathbf{D} - \omega_m \mathbf{I}| = 0. \tag{12}$$

Requiring that Re $\omega_m = 0$, we find the parameter values of λ at marginal stability. Two typical cases are depicted in figure 6.

In both cases a and b shown in the figure, the λ against k curves have extrema, λ_c' and λ_c'', respectively. This means that as λ is varied from values corresponding to asymptotic stability (below curves a and b) to values leading to instability (above curves a and b), the *first* transition will take place at λ_c' or λ_c'' and will therefore dominate the behaviour of the system for nearby values of λ. Now in case a the extremum λ_c' occurs at $k = 0$, that is, at a characteristic spatial length $l = \infty$. This obviously corresponds to a space-independent situation; in other words, the dominant mode in the vicinity of the first bifurcation point will be a homogeneous one. Nevertheless, this mode will have non-trivial properties in the time domain in the sense that, typically, it will have an oscillatory behaviour (Im $\omega \neq 0$ in equation (12)). We may refer to this situation as *time symmetry breaking*, since the oscillatory dynamics will now break the invariance of the reaction–diffusion equations with respect to the phase of the motion.

A new possibility arises when Im $\omega = 0$ in equation (12), and is depicted in figure 6(*b*). Here the extremum λ_c'' occurs at a non-trivial value $k = k_c$, that is, at a well-defined characteristic spatial length $l = l_c$. It follows that the dominant mode in the vicinity of the first bifurcation will now be time independent and spatially inhomogeneous. Moreover, its charcteristics will be *intrinsic*, in the sense that they will be determined entirely by the system's parameters. We are thus entitled to refer to this situation as *space symmetry breaking*.

A much studied model, known as the Brusselator, illustrates these phenomena:

$$\begin{aligned} &\mathrm{A} \rightarrow \mathrm{X} && \text{(R1)} \\ &\mathrm{B} + \mathrm{X} \rightarrow \mathrm{Y} + \mathrm{C} && \text{(R2)} \\ &2\mathrm{X} + \mathrm{Y} \rightarrow 3\mathrm{X} && \text{(R3)} \\ &\mathrm{X} \rightarrow \mathrm{D} && \text{(R4).} \end{aligned} \tag{13}$$

In this reaction, species X produces Y in R2 which in turn activates the production of X

in R3. Reactions R2 and R3 will be accelerated if the concentration of B increases. In rescaled variables, the reaction–diffusion equations are

$$\begin{aligned} \partial X/\partial t &= A - (B+1)X + X^2Y + D_1\nabla^2 X \\ \partial Y/\partial t &= BX - X^2Y + D_2\nabla^2 Y. \end{aligned} \tag{14}$$

The stationary state is

$$X_0 = A \qquad Y_0 = B/A. \tag{15}$$

Assuming a time-independent structure (Im $\omega = 0$ in equation (12)), fluctuations around this uniform state are of the form

$$X(r) = X_0 + x(r) \qquad Y(r) = Y_0 + y(r) \tag{16a}$$

with

$$x(r), y(r) \approx \mathrm{e}^{-r/l_{\mathrm{corr}}} \cos 2\pi r/l_{\mathrm{c}} \tag{16b}$$

in a one-dimensional system. l_{corr} is the correlation length of the fluctuation, i.e. the distance over which a point-like perturbation will spread. l_{c} is the spatial period of the oscillations which modulate the decaying envelope of the perturbation. Solving the linearized equation (10) allows one to determine these lengths as [1]

$$l_{\mathrm{corr}} \simeq [4D_1/(B_{\mathrm{c}} - B)]^{1/2} \tag{17a}$$

$$l_{\mathrm{c}} \simeq 2\pi(D_1D_2)^{1/4}/A^{1/2} \tag{17b}$$

for the concentration B near and below the critical concentration

$$B_{\mathrm{c}} = [1 + A(D_1/D_2)^{1/2}]^2. \tag{18a}$$

When this critical value is reached, the correlation length, equation (17*a*), diverges and the uniform state becomes unstable with respect to fluctuations of the form (16*b*), which grow and invade the system. This stationary instability may be in competition with an oscillatory instability (Im $\omega \neq 0$ in equation (12)) occurring at the critical parameter value

$$B_{\mathrm{c}}' = 1 + A^2. \tag{18b}$$

A detailed study of the characteristic equation (equation (12)) for this model shows that for $D_1 \geqslant D_2$ or for $D_2 > D_1$ and $2\sqrt{D_1D_2}/(D_2 - D_1) > A$, the oscillatory instability occurs before the stationary one and a spatio-temporal structure emerges rather than the stationary, space-symmetry-breaking Turing structure. In other words, stationary patterns may arise as a result of a symmetry-breaking instability of the homogeneous state only if the diffusion coefficient of the 'inhibitor' Y is sufficiently large compared with the diffusion coefficient of the 'activator' X. This imposes constraints on both the chemical mechanism and on the nature of the medium in which it is embedded. Now, in a typical chemical system giving rise to self-organization and chaos, such as the Belousov–Zhabotinski reagent in liquid solution, these constraints are not satisfied since the active species involved are molecules of comparable sizes and, consequently, of comparable diffusion coefficients. This is at the origin of the fact that for a long time most of the experimentally observed dissipative structures were spatio-temporal. The two most characteristic examples known to date are the target patterns and the spiral waves of chemical activity observed in the Belousov–Zhabotinski reagent [12].

Quite recently inhomogeneous states displaying the principal properties of stationary, space-symmetry-breaking Turing structures have been observed thanks to the design of new open, unstirred chemical reactors allowing for the development of spatially inhomogeneous states while avoiding parasitic hydrodynamic motion [13]. Figure 7 depicts the gel reactor designed by De Kepper and co-workers. The two opposite long edges are respectively in contact with two chemical reservoirs A and B where the concentrations of reactants are kept constant and uniform by appropriate mixing and a continuous flow of fresh solutions. The reactants are separated in such a way that neither solution A nor solution B is individually reactive: the chemicals diffuse from the edges into the gel where the reaction takes place. The typical diffusion time to establish stationary concentration profiles across the gel strip is about three hours. The chemical system selected is a variant of the chlorite–iodide reaction in which malonic acid is added, which is known to exhibit a rich dynamical behaviour. To make the concentration changes visible, the gel is loaded with a starch-like colour indicator which does not diffuse through the gel. The colour changes from yellow to blue with the change of the $[I_3^-]/[I_2]$ ratio during the redox reaction. The colour pattern is monitored with a video camera.

At the beginning of the experiment, the development of a series of clear and dark stripes parallel to the edges reveals the emergence of a concentration pattern in the central region of the reactor. Although this pattern is non-trivial, the stripes preserve the symmetry imposed by the feed. But over a well defined range of the malonic acid concentration in A, some of these stripes ultimately break up into lines of periodic spots depicted in figure 8. This constitutes a genuine symmetry-breaking phenomenon in the direction transverse to the imposed gradient. A similar line of spots parallel to the main front has been obtained in a numerical study of the Turing bifurcation of the Brusselator in analogous conditions. The pattern can be sustained indefinitely and is actually found to remain unchanged for more than 20 h. Moreover, the wavelength $l_c \simeq 0.2$ mm seems to be really intrinsic and exclusively characterized by non-geometric properties; in particular, it is much smaller than any geometric size of the reactor (including thickness) by at least one order of magnitude.

One plausible explanation of the appearance of a stationary pattern in this reactor is that small differences in diffusion coefficients (which would be insufficient for the Turing instability to occur in a liquid reagent) are enhanced by the diffusion process in the gel. This is corroborated by recent theoretical developments on reaction–diffusion processes in complex systems [14] and highlights the important role played by the host medium in chemical dynamics.

4. Non-linear behaviour: large systems and universal aspects

We now come to the non-linear behaviour prevailing beyond the instability threshold. In a system of small spatial extension the spectrum of admissible values of the wavenumber k in the linear stability diagram (figure 6) is discrete. As a result, for λ slightly above λ_c' or λ_c'' only the mode corresponding to an admissible k-value close to k_c will be unstable. This problem can be handled by classical methods of bifurcation theory or singular perturbation theory, which allow one to compute the saturation values of the amplitude reached thanks to the non-linear contributions. For instance, in the Brusselator model (equations (14)) one obtains, in one space dimension and zero-flux boundary conditions,

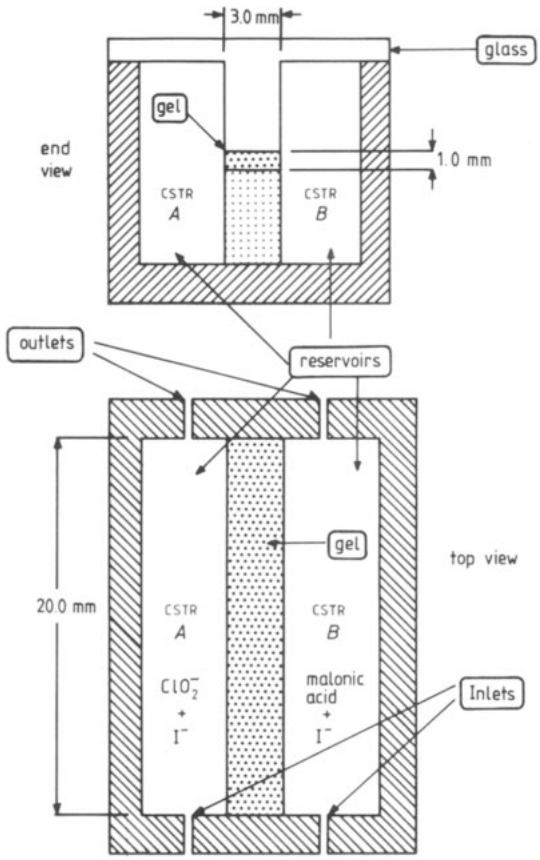

Figure 7. Gel reactor used in [13] for the realization of stationary spatial patterns. The gel strip is fixed between two flat plates 1 mm apart. Reactants are fed through the well-mixed reservoirs A and B.

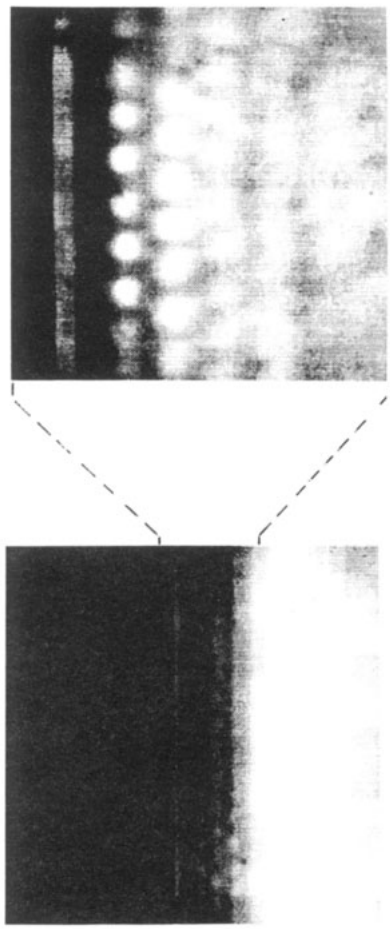

Figure 8. Enlarged image of the region of the reactor, figure 7, in which the pattern is appearing. Distances are in mm. Dark regions correspond to reduced states, clear ones to oxidized states.

the following result for the space independent patterns for values of B close to B_c (equation (18*a*)) [15]:

$$\begin{pmatrix} x(r) \\ y(r) \end{pmatrix} = \left(\frac{B - B_c}{u}\right)^{1/2} \begin{pmatrix} c_x \\ c_y \end{pmatrix} \cos \frac{2\pi}{l_c} r$$

where u, c_x, c_y are constant. Depending on the sign of u the bifurcation is supercritical or subcritical.

A remarkable feature, shared by large classes of non-linear systems giving rise to instabilities, is that, in the vicinity of the threshold, the dynamics can be cast in a universal *normal form* [3] featuring a privileged combination of the initial variables to which we refer as the *order parameter*. In the vicinity of a symmetry-breaking instability leading

to a Turing structure this parameter is, essentially, the amplitude z of the critical mode, and the normal form equation reads

$$dz/dt = (\lambda - \lambda_c)z - uz^3. \tag{19}$$

As the length L of the system is increased an increasing number of modes approach k_c (figure 6) and become simultaneously unstable. This results in several coexisting non-uniform states which may interchange their stability, resulting in *bifurcation cascades*. The latter may culminate in an aperiodic regime to which we refer as *diffusion-induced chaos* [16]. The length L of the system (also called the aspect ratio) is thus an important bifurcation parameter. A similar situation arises in hydrodynamics, where by varying the aspect ratio one may produce a large variety of patterns differing both in wavelength and in shape.

The mathematical description of the above cascading bifurcation phenomena becomes more involved. In many cases one can cast the evolution in terms of normal forms, which then involve more than one order parameter. As a rule the universality of these normal forms can no longer be guaranteed, in the sense that a slight perturbation of the dynamics may introduce new types of behaviour not accounted for in the original normal form [3].

In the limit of a system of large spatial extension the spectrum of k-values in the linear stability diagram (figure 6) becomes continuous. As a result, for any value of λ above criticality, however small $|\lambda - \lambda_c|/\lambda_c$ might be, an infinite number of coupled unstable modes will be switched on. Extensive studies carried out during the last few years show that the principal consequence of this new situation is that the order parameters z satisfying classical normal form equations for small systems (equation (19)) are now becoming slowly varying functions of space and time. The concentration vector $\boldsymbol{x}$ (cf equation (9)) may thus be written near criticality as

$$\boldsymbol{x}(\boldsymbol{r}, t) = \underbrace{z(\varepsilon^{\alpha}\boldsymbol{r}, \varepsilon^{\beta}t)}_{\text{slow variation}}\, \boldsymbol{c}\, \underbrace{\varphi_{k_c}(\boldsymbol{r})\, e^{i m \omega_{k_c}}}_{\text{fast variation}} \tag{20}$$

where $\varepsilon = (\lambda - \lambda_c)/\lambda_c$ and the exponents α and β are to be determined.

Inserting (20) into equation (7) and solving perturbatively for small ε one obtains an equation of evolution for z which turns out to be, typically, a Landau–Ginzburg-type equation, familiar from phase transition theory, for a *complex* order parameter [17]. As an example, if the transition to instability occurs through Im $\omega_{k_c} \neq 0$ the equation for z has the form (in suitably scaled variables and parameters)

$$\partial z/\partial t = \mu z + (1 + i\alpha)\nabla^2 z - (1 + i\beta)|z|^2 z. \tag{21}$$

An alternative approach, developed especially by Kuramoto [16, 18], is to characterize the modulation of the patterns by a slowly varying phase ψ, which may be viewed as the amplitude of the 'Goldstone mode' associated with the symmetry-breaking pattern present:

$$\boldsymbol{X}(\boldsymbol{r}, t) = \boldsymbol{X}_c(\psi(\boldsymbol{r}, t)) + \boldsymbol{b}(\boldsymbol{r}, t) \tag{22}$$

where $\boldsymbol{X}_c$ and $\boldsymbol{b}$ are, respectively, the slowly and rapidly varying parts of $\boldsymbol{X}$. Inserting (22) into equation (7) one obtains, for various orders of perturbation theory, a set of linear inhomogeneous equations, similar to those arising in the Chapman–Enskog solution of

the Boltzmann equation. The solvability condition for these equations leads then to a closed-form equation for the phase:

$$\partial\psi/\partial t = \Omega(\psi, \nabla\psi, \nabla^2\psi, \ldots) \tag{23a}$$

with

$$\boldsymbol{b} = \boldsymbol{b}(\psi, \nabla\psi, \ldots). \tag{23b}$$

The explicit form of (23*a*) depends on the parameters. For instance, in the range of stability of the uniform limit cycle solution one gets a non-linear phase diffusion equation [19]:

$$\partial\psi/\partial t = D\nabla^2\psi + \mu(\nabla\psi)^2 \qquad D > 0 \tag{24a}$$

whereas otherwise one obtains the Kuramoto–Shivashinsky equation,

$$\partial\psi/\partial t = D\nabla^2\psi - D'\nabla^4\psi + \mu(\nabla\Psi)^2 \qquad D < 0, D' > 0. \tag{24b}$$

The study of equations (20)–(24) has attracted wide interest over the last few years. Extensive numerical simulations have been carried out, which have revealed a number of important and unexpected features:

(i) Beyond the instability of the uniform limit cycle solution, equation (24*b*) gives rise to *diffusion-induced phase turbulence*. Although the dimensionality of the attractor describing this regime is very high for a large system, it has been shown that there exists, nevertheless, a finite-dimensional *inertial manifold* in which this attractor can be embedded without loss of its principal qualitative properties [20]. This type of result still remains to be established for fluid dynamical turbulence as described by the Navier–Stokes equation. We find here another feature that makes chemical kinetics special among other fields of science giving rise to self-organization and chaos.

(ii) The patterns generated by equations (20)–(24) often exhibit *defects* [17]. The core of the defect is the place where a change of structure occurs, and corresponds in two dimensions to a line or to a point. In stationary patterns the point defect may be a dislocation in which, say, an extra pair of rolls is inserted in a roll pattern, whereas the line defect may delimit regions with different roll orientations. In time-dependent patterns the analogue of the dislocation is a spiral wave. All these features have been reproduced by numerical solutions of the appropriate equations for the order parameter: for instance, the spiral defect is found to be a solution of the complex Landau–Ginzburg equation (equation (21)). One has, therefore, an appealing interpretation of the experiments on chemical waves. There is strong evidence that in the two-dimensional version of the Kuramoto–Shivashinski equation (equation (24*b*)), phase turbulence may be mediated by defects. In this respect an elegant theory has been elaborated quite recently [21], which describes defects as objects (analogous to 'quasi-particles') evolving and interacting with each other in the effective medium constituted by the phase field. It can be expected that this description may lead to a better understanding of defect-mediated turbulence, at least in some limiting cases involving, for example, a dilute gas of defects.

As was the case in small systems, one finds here an even greater multiplicity of coexisting solutions. The selection of the most stable pattern is sometimes mediated by a variational principle, in particular when the transition to instability occurs through real eigenvalues ($\omega_{k_c} = 0$ in equation (20)) [22]. However, in most cases the equations for the order parameters involve non-variational terms, which actually arise as a result of

the non-equilibrium constraints driving the dynamics of the system. The presence of such terms considerably complicates the problem of selection, which remains largely open.

An unexpected consequence of non-variational effects is the formation of *localized* stable stationary structures, discovered recently by Thual and Fauve in a numerical simulation of the complex Landau–Ginzburg equation [23] in the domain of a subcritical Hopf bifurcation (in which case equation (21) must actually be completed by terms of fifth order in z). In a more chemical context, it has been shown by Dewel and Borckmans [24] that similar behaviour may arise in activator–inhibitor systems in which the fast-diffusing inhibitor may block the further spread of the activator and confine it in a limited region of space. Further aspects of this remarkable stabilization of a 'droplet' of a new state embedded in a 'reference' unstable state have been studied by Hakim *et al* [25].

5. Microscopic aspects of chemical instabilities

As stressed repeatedly throughout the present paper, the very possibility of self-organization in chemistry implies the existence of characteristic lengths of intrinsic origin over which macroscopic order can be extended. This automatically raises a conceptual problem, since chemical reactions result from the action of short-range forces, extending over microscopic characteristic lengths.

In this section we discuss briefly how the onset of macroscopic order is reflected at the molecular level. To this end we set up an augmented description of chemical dynamics incorporating thermodynamic fluctuations, viewed as a random process. We also consider alternative sources of randomness, such as the stochastic perturbations that the environment inflicts on a real-world system, and examine their role in the mechanism of the instability and in the selection of the states above criticality.

Without going into technical detail we recall here that there are two methods allowing one to analyse the effect of fluctuations or external random perturbations [1]: the *Master equation* description in which one incorporates detailed information on the individual processes involved in the stochastic dynamics, and the *generalized Langevin equation* approach in which stochastic effects are accounted for globally by adding random force terms in the equations of evolution. One can show that below and up to a small neighbourhood of the bifurcation point λ_c both formalisms are equivalent and describe the augmented dynamics as a first-order Markov process. This allows one to compute the spatial correlation function of the fluctuations $\boldsymbol{x}(\boldsymbol{r}, t)$ around the (uniform) reference state $\boldsymbol{X}_0$. The result reads (taking for simplicity the autocorrelation function of a single variable x)

$$\langle x(\boldsymbol{r}, t)x(\boldsymbol{r}', t)\rangle = X_0\delta(\boldsymbol{r} - \boldsymbol{r}') + g(\boldsymbol{r}, \boldsymbol{r}') \tag{25a}$$

with [26]

$$g(\boldsymbol{r}, \boldsymbol{r}') = aJg(|\boldsymbol{r} - \boldsymbol{r}'|/l_{\text{corr}}). \tag{25b}$$

Here a is a numerical coefficient, J the mass flux across the system, and l_{corr} a macroscopic length having the structure anticipated in the introduction of which equation (17a) constitutes a concrete illustration for the Brusselator model.

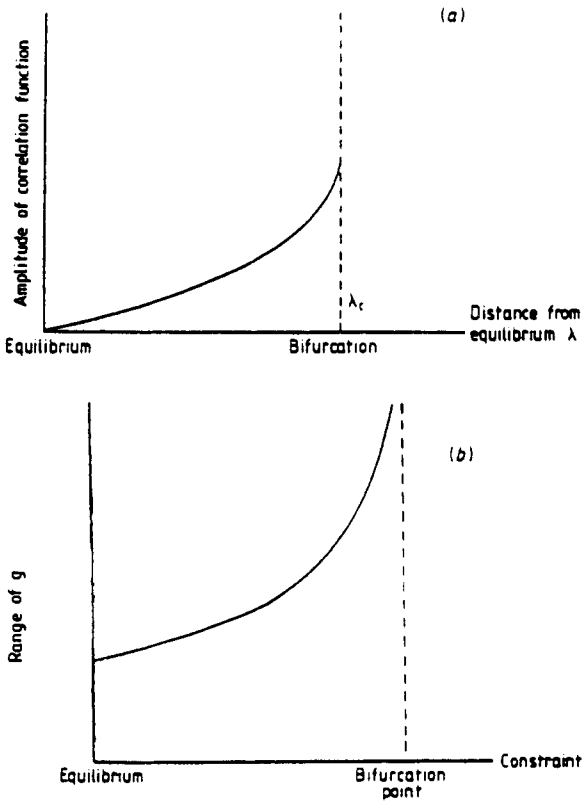

Figure 9. Typical dependence of the amplitude (*a*) and range (*b*) of the correlation function g (equation (25*b*)) of a chemical system as a function of the non-equilibrium constraint.

Figure 9 depicts the dependence of the amplitude (J) and range (l_{corr}) of the correlation function as a function of the distance from equilibrium, a privileged control parameter for most dissipative systems. At equilibrium the correlation function vanishes ($J = 0$), and equation (25*a*) reduces to the classical equilibrium result, that the statistics of the fluctuations in an ideal system are Poissonian. On the other hand l_{corr} remains finite at equilibrium but its effect is masked by the vanishing of the amplitude. As soon as the system deviates from equilibrium J becomes non-zero and fluctuations of macroscopic range are set up in the system. One is, therefore, entitled to assert that non-equilibrium is, above all, a *correlated state of matter*.

One interesting consequence of correlations of macroscopic range is seen when equation (25*a*) is integrated over a volume element ΔV and the variance $\langle(\delta x)^2\rangle$ is evaluated. One obtains

$$\langle(\delta x)^2\rangle_{\Delta V} = X_0 + \mathrm{O}(\Delta V/V) \tag{26}$$

implying in particular that locally ($\Delta V/V \to 0$) fluctuations remain Poissonian, whereas globally ($\Delta V/V \to 1$) macroscopic deviations from the Poissonian must be expected. This theoretical prediction has recently been verified by microscopic (molecular dynamics) simulations of simple, one-variable reaction schemes [27]. It would be very interesting to detect this effect in laboratory experiments as well.

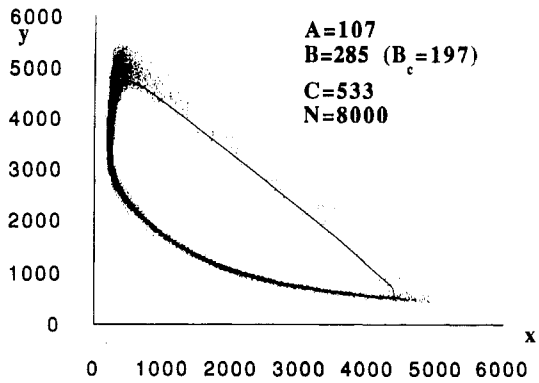

Figure 10. Periodic behaviour of the Brusselator as deduced from the solution of the phenomenological reaction–diffusion equations (full curve) and from a microscopic simulation (dots).

When the system approaches a bifurcation point the correlation length tends to diverge (figure 9(*b*)), a property reflecting the intuitive idea that order must indeed encompass the entire system and drive it coherently to the new regime arising beyond the instability. In reality the situation is much subtler. Firstly, as pointed out in section 4, in systems of large spatial extension there exist a continuum of interacting modes, giving rise to a large variety of patterns; secondly, in the presence of fluctuations these different states are mixed and it may happen that the macroscopic order parameter is averaged out to zero.

These questions have been discussed intensively in the literature in recent years. We do not enter into the technical detail of these, partly open, questions [22, 28] here. Instead, we stress the need for microscopic simulations and laboratory experiments on bifurcation phenomena and, in particular, the need to assess the role of the fluctuations. An encouraging result in this direction has been obtained recently by Mareschal and De Wit, who performed a direct Monte Carlo simulation of the Brusselator [29]. Figure 10 summarizes their main result in the range of parameter values in which the phenomenological description predicts a Hopf bifurcation leading to a limit cycle. We see that the microscopic dynamics follows the macroscopic oscillation for several periods, in other words, that macroscopic order is not destroyed by the fluctuations. More work is necessary on the role of spatial dimensionality, of the size of the system and of the distance from bifurcation before it can be claimed that a satisfactory microscopic theory of chemical self-organization is available.

References

[1] Nicolis G and Prigogine I 1977 '*Self-organization in Non-equilibrium Systems*' (New York: Wiley) p 491
[2] Gray P, Nicolis G, Baras F, Borckmans P and Scott S (ed) 1990 '*Spatial Inhomogeneities and Transient Behaviour in Chemical Kinetics*' (Manchester: Manchester University Press) p 756
[3] See for instance,
Guckenheimer J and Holmes Ph 1983 '*Nonlinear Oscillations, Dynamical Systems and Bifurcations of Vector Fields*' (Berlin: Springer) p 453
[4] Sil'nikov L P 1965 *Sov. Math.–Dokl* **6** 163; 1970 *Math. USSR Sbornik* **10** 91
[5] Gaspard P and Nicolis G 1983 *J. Stat. Phys.* **31** 499
[6] Gaspard P, Kapral R and Nicolis G 1984 *J. Stat. Phys.* **35** 697
Glendinning P and Sparrow C 1984 *J. Stat. Phys.* **35** 645
[7] Feigenbaum M 1978 *J. Stat. Phys.* **19** 25
[8] Showalter K, Noyes R and Bar-Eli K 1978 *J. Chem. Phys.* **69** 2514

[9] Argoul F, Arneodo A and Richetti P 1987 *Phys. Lett.* **201A** 269
[10] Bassett M and Hudson J 1988 *J. Phys. Chem.* **92** 6963
[11] Turing A 1952 *Phil. Trans. R. Soc.* B **237** 37
[12] See, e.g.
Field R and Burger M (ed) 1985 '*Oscillations and Travelling Waves in Chemical Systems*' (New York: Wiley) p 681
[13] Castets V, Dulos E, Boissonade J and De Kepper P 1990 *Phys. Rev. Lett.* in press
[14] Nicolis G and Altares V 1989 *J. Phys. Chem.* **93** 2861
[15] Auchmuty J and Nicolis G 1975 *Bull. Math. Biol.* **37** 323
Herschkowitz-Kaufman M 1975 *Bull. Math. Biol.* **37** 585
[16] Kuramoto Y 1984 '*Chemical Oscillations, Waves and Turbulence*' (Berlin: Springer) p 156
[17] See, e.g.,
Lega L 1990 Defects and defect-mediated turbulence, ed D Walgraef and N Ghoniem '*Patterns, Defects and Materials Instabilities*' (Dordrecht: Kluwer Academic) p 393
[18] Kuramoto Y 1990 Extended phase dynamics approach to pattern evolution '*Spatial Inhomogeneities and Transient Behaviour in Chemical Kinetics*' ed P Gray, G Nicolis, F Baras, P Borckmans and S Scott (Manchester: Manchester University Press) p 756
[19] Ortoleva P and Ross J 1972 *J. Chem. Phys.* **58** 5673
[20] Constantin P, Foias C, Nicolaenko B and Temam R 1989 '*Integral Manifolds and Inertial Manifolds for Dissipative Partial Differential Equations*' (Berlin: Springer) p 121
[21] Rica S and Tirapegeui E 1990 *Phys. Rev. Lett.* **64** 878
[22] Walgraef D, Dewel G and Borckmans P 1982 *Adv. Chem. Phys.* **49** 311
[23] Thual O and S Fauve S 1988 *J. Physique* **49** 1829
[24] Dewel G and Borckmans P 1990 'Localized structures in reaction–diffusion systems' '*Patterns, Defects and Materials Instabilities*' ed D Walgraed and N Ghoniem (Dordrecht: Kluwer Academic) p 393
[25] Hakim V, Jacobsen P and Pomeau Y 1990 *Europhys. Lett.* **11** 19
[26] Nicolis G and Malek-Mansour M 1984 *Phys. Rev.* A **29** 2845
[27] Nicolis G, Amellal A, Dupont G and Mareschal M 1989 *J. Mol. Liq.* **41** 5
[28] Malek-Mansour M, Vanden Broeck C, Nicolis G and Turner J W 1981 *Ann. Phys., NY* **131** 283
Lemarchand H and Nicolis G 1984 *J. Stat. Phys.* **37** 609
[29] Mareschal M and De Wit A 1990 Microscopic simulation of a chemical instability *J. Chem. Phys.* submitted.